MOLECULAR PHARMACOLOGY, 27:246-255

Triphenylmethylphosphonium Blocks the Nicotinic Acetylcholine Receptor Noncompetitively

C. E. SPIVAK AND E. X. ALBUQUERQUE

Addiction Research Center, National Institute on Drug Abuse, Baltimore, Maryland 21224 (C.E.S.) and Department of Pharmacology and Experimental Therapeutics, University of Maryland School of Medicine, Baltimore, Maryland 21201 (E.X.A.)

Received September 25, 1984; Accepted November 5, 1984

SUMMARY

Triphenylmethylphosphonium (TPMP) blocked the nerve-elicited twitch tension of frog sartorius muscles by 50% at a concentration of about 20 μM. This neuromuscular blockade by TPMP, which originated at the level of the nicotinic receptor, was due in part to the ability of the drug to block the quiescent receptor by degrees that depended on the TPMP concentration and on membrane potential. In addition, the blockade was markedly enhanced when the receptor was activated by acetylcholine. Finally, TPMP shortened the lifetimes of ACh-activated ion channels. These findings were interpreted as follows. Under resting conditions, TPMP shifted the equilibrium of the receptor channel complex toward the desensitized state. TPMP united with the activated ion channel to shorten channel lifetime and to deepen the blockade. High concentrations ($\geq$50 μM) of TPMP altered muscle action potentials and often increased, by about 30-fold, the frequency of miniature endplate potentials.

INTRODUCTION

When ACh[1] binds to its recognition site on the nicotinic receptor of the neuromuscular junction, the receptor's ion channel opens. The resulting current that crosses the cell membrane depolarizes the endplate region and ultimately triggers a twitch in the fiber. This current generated when the AChR is activated can be blocked by a variety of organic cations (1–3).

TPMP is one such cation that has been studied by biochemical methods (4–6). TPMP (10 μM) blocked the efflux of ^{22}Na through the AChR of *Torpedo marmorata* membranes (4), and at concentrations <1mM did not bind to the recognition site of the AChR. It did, however, compete with phencyclidine, which has been shown to be a noncompetitive channel blocking agent at the AChR (Ref. 4; see also Ref. 7). Though TPMP bound to AChR-rich membranes alone, its binding was increased severalfold when nicotinic agonists and antagonists co-incubated with TPMP (4–6). The subunits of the AChR to which TPMP bound were located by activating the AChR with ultraviolet light, which caused TPMP to bind covalently. These experiments showed that a nicotinic agonist or antagonist caused the binding to shift from mostly the α subunit to the δ and β subunits (5, 6).

In addition, it has been shown that carbamylcholine and α-bungarotoxin both enhance the partitioning of spin-labeled analogues of TPMP into the membrane phase of electric organ from *Torpedo californica* (8). Davis *et al.* (9) used an ion-selective electrode to monitor the aqueous concentration of another analogue of TPMP, namely tetraphenylphosphonium, in the presence of membrane vesicles from *T. californica.* They observed that nicotinic agonists and (+)-tubocurarine enhanced the uptake of tetraphenylphosphonium from the aqueous phase.

In the light of the present biochemical findings, we decided to explore the electrophysiological correlates to the uptake studies. We found an agonist-enhanced blockade of the AChR, in qualitative agreement with the biochemical findings. In addition, TPMP shortened channel lifetimes and blocked the AChR in the absence of repetitive stimulation by ACh.

MATERIALS AND METHODS

Chemicals and physiological solutions. The frog Ringer's solution had the following composition (millimolar concentrations): NaCl, 116; KCl, 2.0; $CaCl_2$, 1.8; NaH_2PO_4, 0.7; Na_2HPO_4, 1.3. The pH was 7.1. In EPC experiments, 600 mmol/liter of glycerol was added to the Ringer's solution. Muscles were treated with this solution for 1 hr and then washed for $\geq$1 hr to abolish the twitch (10). In experiments using trains of action potentials, pretreatment with 200 mM glycerol for 1 hr was sufficient to stabilize the fibers without decreasing the resting membrane potential. The Hanks' solution used to bathe rat myoballs and fill patch pipettes had the following composition (millimolar concentrations): NaCl, 137; KCl, 5.4; $NaHCO_3$, 4.2; $CaCl_2$, 1.3; $MgSO_4$, 0.81; KH_2PO_4, 0.44; D-glucose, 5.6. To this was added 10 ml/liter of HEPES

This study was supported in part by ARO Grant DAAG-29-81-K-0161 and United States Public Health Service Grant NS-12063.

[1] Abbreviations used are: ACh, acetylcholine; AChR, the nicotinic receptor ion channel complex; EPC, endplate current; MEPC, miniature endplate current; MEPP, miniature endplate potential, TPMP, triphenylmethylphosphonium; HEPES, 4-(2-hydroxyethyl)-1-piperazineethanesulfonic acid.

0026-895X/85/020246-10$02.00/0

solution (1 M, pH 7.3), and 1 ml/liter of stock tetrodotoxin solution (0.3 mM). Acetylcholine chloride was purchased from Sigma Chemical Company (St. Louis, MO), and triphenylmethylphosphonium bromide was purchased from Aldrich Chemical Company (Milwaukee, WI).

Physiological recording. Twitch tension was recorded from sciatic nerve sartorius muscle preparations of the frog *Rana pipiens*, using Grass FT .03 force displacement transducers. The muscles, under 2–3 g of resting tension, stabilized for ≥30 min in Ringer's solution before the TPMP-Ringer's solution was tested. Directly and indirectly elicited twitches alternated at 0.05 Hz. Preparations were washed for 30 min after each test.

For intracellular recording, sartorius muscles with or without the sciatic nerve were pinned to a Sylgard plate and used for EPC, action potential, and MEPP frequency experiments. Glass microelectrodes were filled with 3 M KCl and had resistances of 1–4 megaohms. For EPC experiments, surface fibers were voltage clamped by a conventional two-microelectrode technique (11). The clamp was established at the junctional region where the EPP rise time was minimal (≤1 msec). The EPC waveforms were sent on line to a PDP 11/40 digital computer for measurement of peak amplitude and estimation of the time constant for decay, as previously described (11, 12). ACh responses were obtained from junctional regions of frog sartorius fibers. The ACh pipettes, which had resistances of >60 megaohms, usually required a braking current of less than 20 nA. Microiontophoretic currents had durations of 0.1 msec. Placement of the ACh micropipette, guided by the amplitude of the depolarizing response and by considerations of stability, usually yielded ACh sensitivities of around 300 mV/nanocoulomb. Recordings of the same cell were made under control condition and in the presence of a concentration of TPMP, 10 bath volumes of which flowed through the bath during the 30 min that preceded recording. Occasionally, the preparation was stable enough to permit washing or testing another TPMP concentration. The recording of action potentials was similar to methods described previously (13). Quantal content was determined by the ratio of EPP amplitude, in the presence of 12 mM Mg^{2+} and 0.9 mM Ca^{2+}, to MEPP amplitude. The same cell was recorded under both control condition and in the presence of TPMP. Waveforms were measured from a digital oscilloscope.

Patch clamp data were derived from rat myoballs, usually 7 to 14 days old, at 21°. Methods and conditions for culturing the myoballs are described elsewhere (14). Some batches of myoballs had distinctly different populations of channels. Those used for this paper, however, were all obtained during the same month and were homogeneous. Patch pipettes, fabricated as described previously (14), had shanks coated with Sylgard or occasionally with Kronig's cement. The current to voltage converting headstage and associated electronics was an EPC-5 unit (List Medical). The current waveforms were filtered at 1 kHz (low pass) through a 4-fold Butterworth characteristic filter, recorded on a Racal Store 4/DS FM tape recorder, and analyzed by computer as detailed previously (14). When channel lifetimes were greatly shortened (to around 5 msec) by TPMP, the tape had to be replayed at ¼ of the recording speed to permit an adequate sampling rate.

RESULTS

TPMP blocked neuromuscular transmission. TPMP blocked neuromuscular transmission progressively so that concentrations as low as 20 μM could block the twitch completely if given enough time (usually over 1 hr). To distinguish the blockade induced by the drug from possible muscle deterioration, and to standardize the method, responses were measured after a 15-min treatment. Fig. 1 shows the concentration response curve taken from 16 muscles. The concentration that blocked the response by 50% was around 20 μM.

TPMP acted postsynaptically in a use-dependent manner. To isolate postsynaptic from presynaptic effects and to determine how stimulation frequency influences junctional ACh sensitivity in the presence of TPMP, ACh was delivered microiontophoretically to junctional regions of frog sartorius fibers. Since a given fiber was used under control, drug, and sometimes washed conditions, stability was more important than high ACh sensitivity. Usual ACh sensitivities were 100–300 mV/nanocoulomb. Trains of ACh pulses were administered at 1, 2, 4, 8, 16, and 32 Hz. Usually no change in postsynaptic response was observed under control conditions. However, in the presence of TPMP (≥30 min) at concentrations as low as 0.5 μM, a significant decrement in the transient depolarizations induced by ACh was recorded that became most evident at higher frequencies of stimulation and higher concentrations of the drug (Fig. 2). The data were complicated by two findings. First, only in the presence of TPMP, we occasionally observed facilitation of the ACh responses, i.e., the responses grew during the first two to four pulses before declining in subsequent ones. This facilitation was usually 110% or less of the first pulse. Second, the decrease in response usually showed a double exponential decrease with time. A multi-exponential decrease is expected under a variety of simple models (see Discussion). This effect is seen in Fig. 2, which is a Guggenheim plot of the response from one cell. The Guggenheim plot is advantageous in confirming single or multiple exponential declines because contamination by the asymptote, which could distort an ordinary semilogarithmic plot, has been removed by subtracting pairs of data points with a constant interval between them (15). Asymptotes for three concentrations are plot-

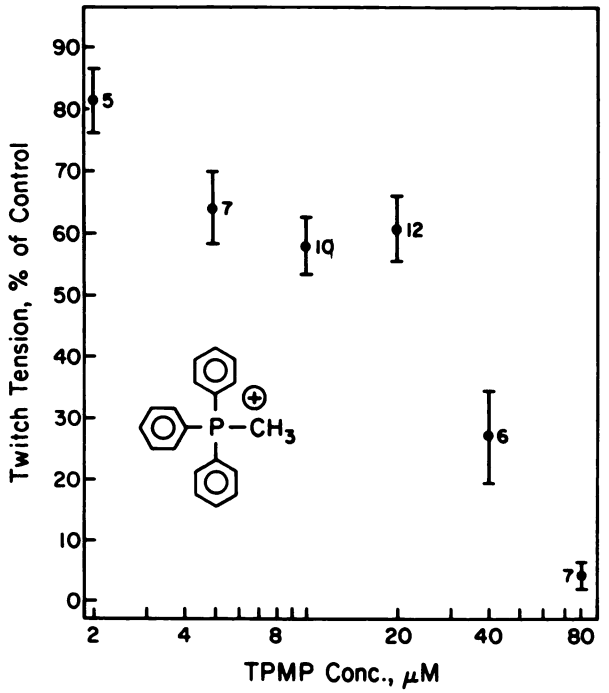

FIG. 1. *Dose-response relationship for nerve-evoked muscle twitches in the presence of TPMP*

Twitch tensions of frog sartorius muscles are plotted as percentage of control after 15 min of treatment. Means ± standard error and the number of muscles tested at each concentration are shown. A total of 16 muscles was used for two or more tests at different TPMP concentrations. The inset shows the chemical structure of TPMP.

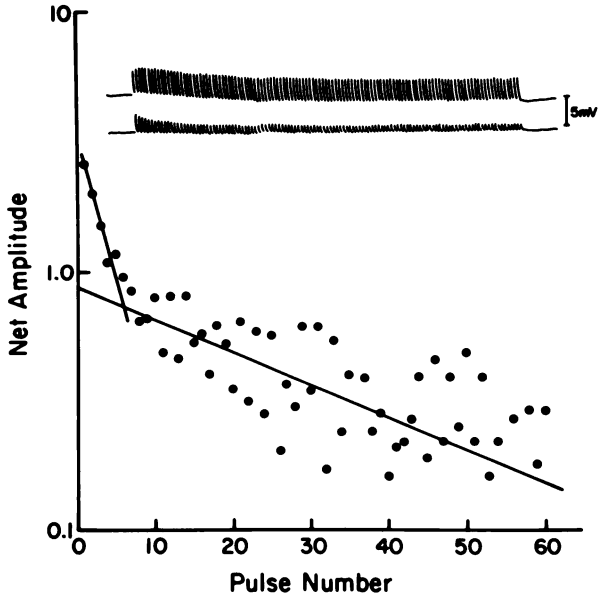

FIG. 2. *Trains of junctional ACh potentials in the absence and presence of TPMP*

In the inset are examples of the ACh potentials obtained at 16 Hz under control condition (upper trace) and in the presence (lower trace) of 2 μM TPMP. ACh was delivered by microiontophoresis with pulse durations of 0.1 msec. The Guggenheim plot was derived from a different fiber in the presence of 10 μM TPMP. The 120 responses were divided in half, and the amplitude of the pulses from the second half were subtracted from the corresponding amplitudes in the first half. The net amplitude (in millivolts) is uncontaminated by the asymptote. The semilogarithmic plot shows that the decline in potentials followed a double exponential time course.

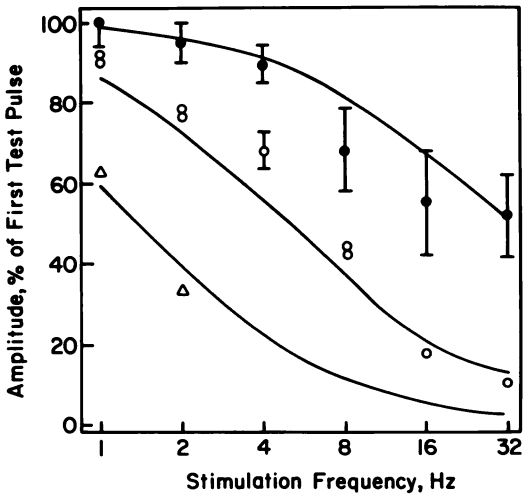

FIG. 3. *Asymptotic ACh potentials after a train of ACh pulses delivered to junctional regions of frog sartorius fibers*

Conditions were as in Fig. 2. By the end of the trains, the ACh responses approached constant values, plotted here for three TPMP concentrations, 1 (●), 10 (○), and 20 μM (△). Error bars represent standards errors for three muscles. Otherwise responses from individual muscles are shown. Though 0.5, 1, and 10 μM TPMP were also tested, their results were omitted here for clarity. The three curves result from the oversimplified model (see text and Appendix) in which the rate constant for recovery is 0.5 sec $^{-1}$ and the fraction of available receptors blocked by each ACh pulse is 1.5, 11, and 45% (top to bottom).

ted against frequency in Fig 3. Data points from other concentrations were omitted for clarity. One sees that even 1 μM produced about a 50% depression in response when ACh was delivered at 32 Hz.

The curves in Fig. 3 were derived (Appendix) for a simple scheme in which a given fraction, f, of the available receptors is blocked by each ACh pulse and recovers with a rate constant, k. This oversimplified scheme, which predicts a single exponential decrease in response, nonetheless fits the asymptote data moderately well. More importantly, it shows that blockade of even a small fraction of receptors with each pulse can greatly diminish the final asymptotic responses.

To evaluate possible presynaptic contributions to the neuromuscular blockade, we performed quantal content experiments in the presence of 10 and 20 μM TPMP. There was no change after incubation for up to 90 min. At higher concentrations some alteration of action potentials was seen (see below), but this would not contribute to the blockade of the neuromuscular junction. We conclude that neuromuscular blockade originated at the level of the AChR.

TPMP blocked closed ion channels in a voltage-dependent manner. In EPC experiments, the membrane potential was routinely changed in 10-mV steps with 3 sec between EPCs. Peak amplitudes are shown under control conditions and in the presence of 20 μM TPMP in Fig. 4A. Whereas under control conditions the plot was nearly linear, in the presence of TPMP there was a clear curvature in the third quadrant. The curvature could be eliminated if the cell was held at −50 mV and the potential changed to various other levels for 10 msec, during which the EPC was triggered (Fig. 4A). Thus, the extent of blockade depended on the membrane potential. Fig. 4B shows that in one cell the approach to equilibrium was an exponential function of time with a time constant of about 3 sec. This time constant varied between frogs. Hyperpolarizing intensified the blockade and depolarizing relieved it. Note at the top of Fig. 4B that, while peak amplitudes changed with time, the time constants for the EPC decays did not. To distinguish between the influence of voltage and stimulation, membrane potentials were changed by ±100 mV for 0.5 sec. EPCs were elicited both before and after but not during the voltage change. Fig. 5 shows that a hyperpolarizing step diminished the EPC peak amplitudes; a depolarizing step increased them (not shown). These results showed that, in the absence of repetitive stimulation, TPMP produced an equilibrium level of blockade that depended on membrane potential, and that shifts in this equilibrium were relatively slow. After washing (1 hr), EPC amplitudes returned to nearly control levels.

TPMP shortened lifetimes of open channels. Under both control conditions and in the presence of TPMP, EPCs decayed as single exponential functions of time (Fig. 6, B and C). The time constants, τ, for these decays were shortened progressively as the TPMP concentration increased, especially at more negative potentials (Fig. 6). Since τ is a reflection of the lifetime of open ion channels under control conditions (16), this finding suggested that TPMP shortened channel lifetime. The sim-

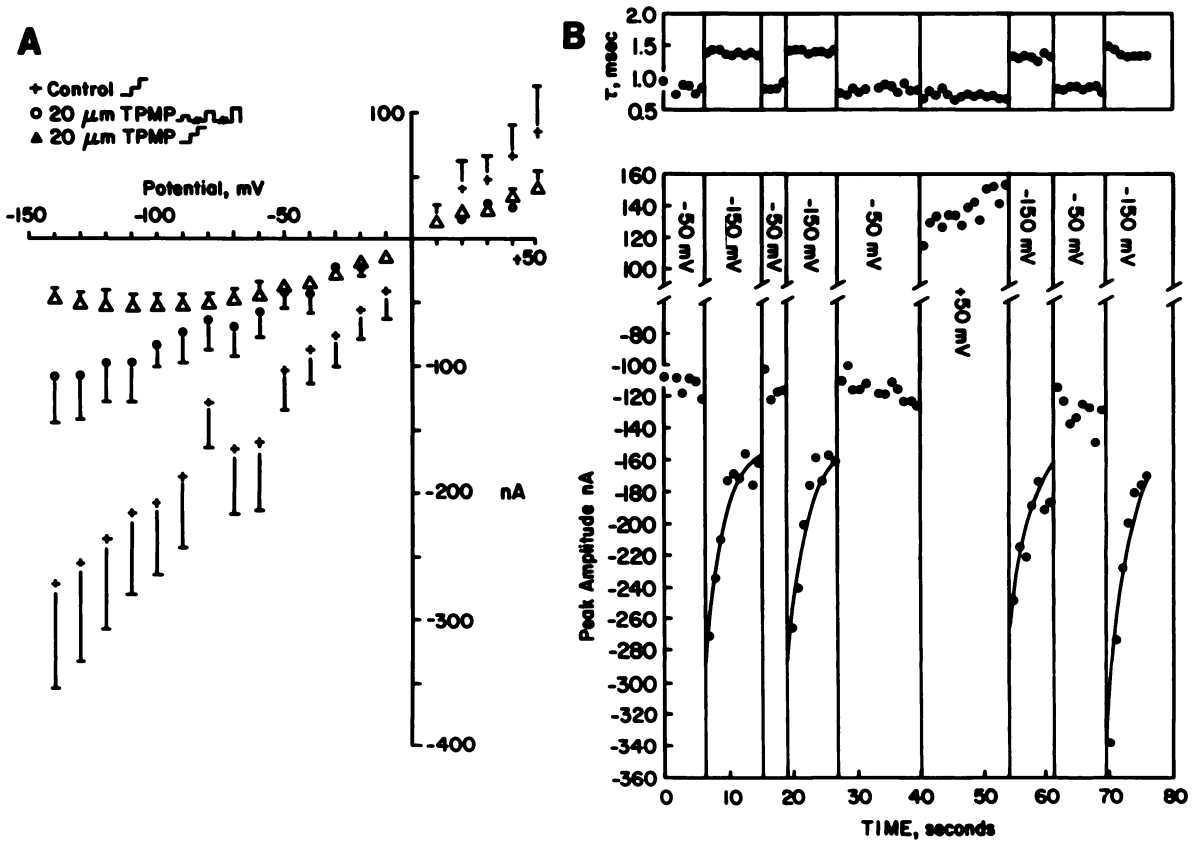

FIG. 4. *TPMP decreased peak amplitudes of EPCs with time and voltage dependence*

In A are shown current-voltage plots of peak amplitudes under control condition (+) and in the presence of TPMP (20 μM). Means and standard errors of 8–22 fibers from 2–3 muscles are shown. When the command potential was changed in 10-mV steps with 3-sec intervals, TPMP induced a marked nonlinearity with zero or negative slope conductance in the third quadrant (Δ). However, when the cell was held at −50 mV and jumped to other potentials for durations of only 10 msec, during which the EPC was elicited, the current voltage relationship returned to linearity (O), but with decreased slope conductance. These experiments showed that the curvature arose from the time voltage dependence in EPC peak amplitudes induced by TPMP. This time voltage dependence is seen more clearly in B. The command potential was changed as shown and EPCs were elicited at 1 Hz. After a hyperpolarizing step, peak amplitudes first increased with the increased driving force and then declined with an approximately exponential time course. All the drawn curves are exponential functions of time with maxima shown, with time constants of 3 sec and with asymptotes of −150 nA. Depolarizing the fiber to +50 mV partially reversed the blockade. Despite this voltage and time dependence seen in the peak amplitudes, the time constants for the decays (B, upper panel) were *independent* of time and voltage. Data for A and B were from different series of experiments. All the data in B were from a single fiber.

plest scheme to account for this finding is the sequential model that is discussed at length elsewhere (e.g., Refs. 1–3). Briefly stated, the open channel closes by two routes, namely by spontaneous, normal closure and by union with TPMP:

$$AR \underset{\alpha}{\longleftarrow} AR^* \xrightarrow[k]{D} ARD$$

Here AR is the agonist-receptor complex, AR^* denotes the open channel conformation, and D represents TPMP. Since the decays were single exponential functions of time, the reverse reaction, $ARD \rightarrow AR^* + D$, was too slow to contribute to the EPC. Thus, the observed rate constant for channel closure, $1/\tau$, is the sum of the two rate constants for egress from the activated state, namely $1/\tau = \alpha + k[D]$. Plots of $1/\tau$ vs. $[D]$ were linear (Fig. 7A), as expected from this model, with slopes that were estimates of the rate constants, k. The k values, which diminished as membrane potential became more positive, ranged from 2.15×10^7 M^{-1} sec^{-1} at −150 mV to 0.76×10^7 M^{-1} sec^{-1} at +50 mV. These values were similar to those found for the variety of other compounds that also seem to block the open ion channel (see Table 4 in Ref. 3). The systematic decrease in k is shown as a plot of ln k vs. membrane potential in Fig. 7B. Since ln k is proportional to the free energy for activation of the TPMP-binding reaction, one sees that an electrostatic component, proportional to membrane potential, adds to the free energy. The calculated fraction, δ, of the membrane electric field sensed by the cation TPMP at its rate-limiting energy barrier estimated from the slope of the plot in Fig. 7B (1, 2) was 8%.

A decrease in channel lifetime could be visualized directly in patch clamp experiments performed on cultured rat myoballs (Fig. 8). One can see that channel currents were usually rectangular pulses under control condition and, though shorter, in the presence of TPMP. This finding is consistent with the model for blockade of the open ion channel described above. Under control condition and in the presence of TPMP, histograms of lifetimes of open channels were largely fitted by a single

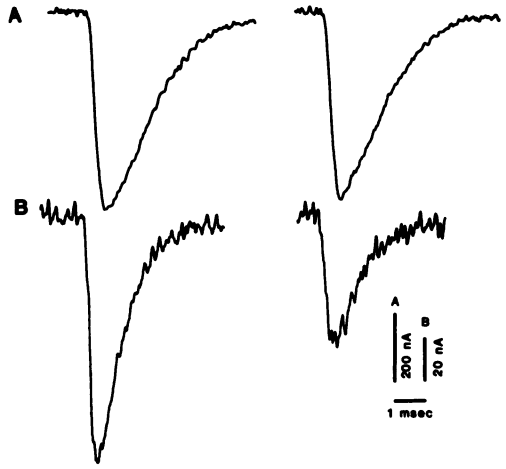

FIG. 5. *EPCs (at −50 mV) before (left) and after (right) a voltage jump of 500-msec duration to −150 mV*

The EPCs were elicited 12 msec after the voltage jump finished. The traces in A were from a fiber under control condition, whereas those in B were from a fiber (same muscle) treated with 20 μM TPMP. Since no EPCs were elicited during the voltage jump, this experiment showed that the voltage-time dependence depended on the voltage jump alone. Note that the time constant for the decay is seen to be shorter in B than in A (see Fig. 6).

exponential distribution, though frequently the first one or two bins exceeded the curve (Fig. 9). We used arithmetic means to characterize the two conditions. When conductance levels were determined, it seemed clear that TPMP had little or no effect. No population of low conductance channels appeared, as it did when pyridostigmine was used (14). To accommodate the variety of recording conditions that we used in these experiments (pipette potentials, cell attached versus cell free, various membrane potentials), we plotted mean channel lifetime versus channel amplitude in Fig. 10. It is evident that the lifetime was not only reduced, but also that its dependence on membrane potential was decreased. In terms of the open channel blockade mechanism, channels were blocked faster when currents were greater, i.e., at more hyperpolarized potentials.

Effects of high concentrations of TPMP. Although the primary focus of this work was on the effects of TPMP at the AChR, we found that high concentrations (50–100 μM) could also affect action potentials and MEPP frequency.

The falling phase of the action potential was most sensitive to TPMP. The maximum rate of fall was decreased from the control level, 200 ± 8 V/sec (standard error; $v = 35$), to 178 ± 8 V/sec ($n = 24$) in the presence of 50 μM TPMP. Threshold, amplitude, and maximum rate of rise were unchanged at this concentration. At 100 μM) the maximum rate of fall decreased further to 116 ± 5 V/sec ($n = 26$), and small decreases in amplitude and the maximum rate of rise also appeared. Repetitive stimulation of glycerol-shocked muscle further slowed the maximum rate of fall, and it prolonged the refractory period, as seen in Fig. 11. Delayed rectification experiments (17) indicated that part of the prolongation of the action potential could be attributed to blockade of potassium channels (data not shown). The effects of TPMP on action potentials were unchanged by >2 hr of washing, suggesting that TPMP either remained at its binding site or that it produced irreversible alterations.

In some muscles, transient bursts of high frequency MEPPS were occasionally seen at 20 μM and lower concentrations of TPMP. To exaggerate this effect, muscles were treated with 100 μM TPMP for 1 hr. In 8 of 12 muscles tested, a roughly 30-fold increase in MEPP frequency appeared, usually during the subsequent wash (Fig. 12). This increase in MEPP frequency could be due to the liberation of calcium from intracellular stores in the presynaptic nerve terminal. We did not investigate this phenomenon further, however, because of the high concentration of TPMP required and the variability of its effects.

DISCUSSION

We have shown that TPMP blocks neuromuscular transmission at the AChR. The blockade appeared in

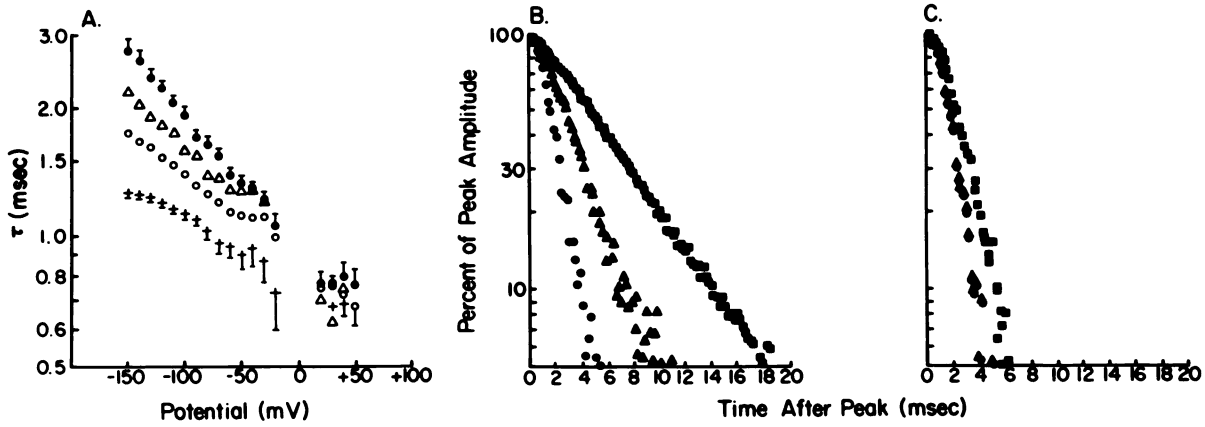

FIG. 6. *The time constants (τ) for decays of EPCs were shortened by TPMP*

In A, the time constants (means ± standard errors for 8–13 fibers from 3 muscles) are plotted as a function of membrane potential under control condition (●) and in the presence of 5 (△), 10 (○), and 20 (+) μM TPMP. Representative standard errors are shown as bars. Panels B and C show representative semilogarithmic plots of the decay phases of EPCs under control condition (B) and in the presence of 20 μM TPMP (C). Membrane potentials were −150 (■), −50 (▲), and +50 (●) mV. The linear plots showed no trace of admixture with a second component.

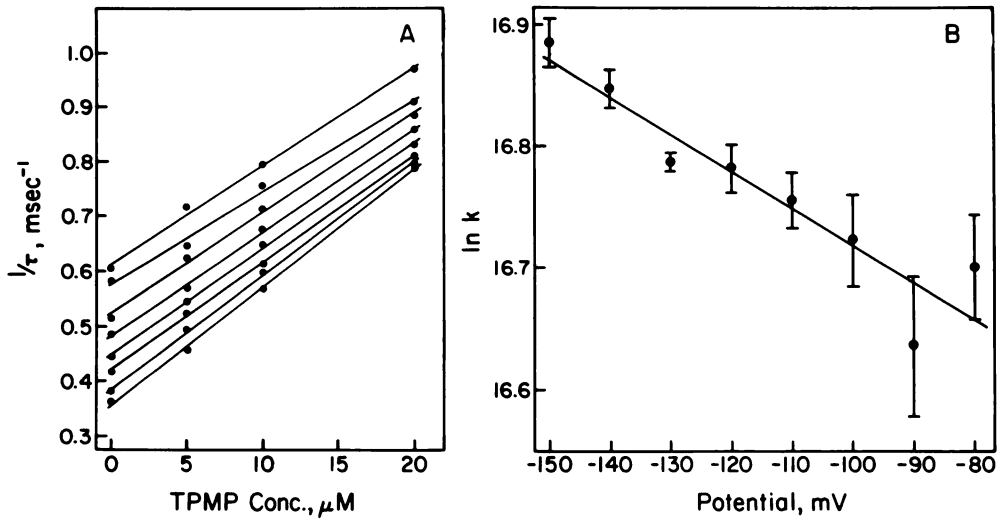

FIG. 7. *Rate constants for EPC decays*

In A are shown the mean values of $1/\tau$ (from Fig. 6) plotted as functions of TPMP concentration. The membrane potentials were −150 to −80 mV (bottom to top) increasing by 10-mV increments. The slopes of these lines, estimates of the rate constants, k, for union of TPMP with the AChR (see text), are plotted in B against membrane potential (semilogarithmic plot). The dependence of ln k on potential indicates, under the model described in the text, that TPMP senses about 8% of the transmembrane electric field at its rate-limiting energy barrier. The error bars shown in B were estimates of the standard deviation in slope obtained from the regression lines shown in A.

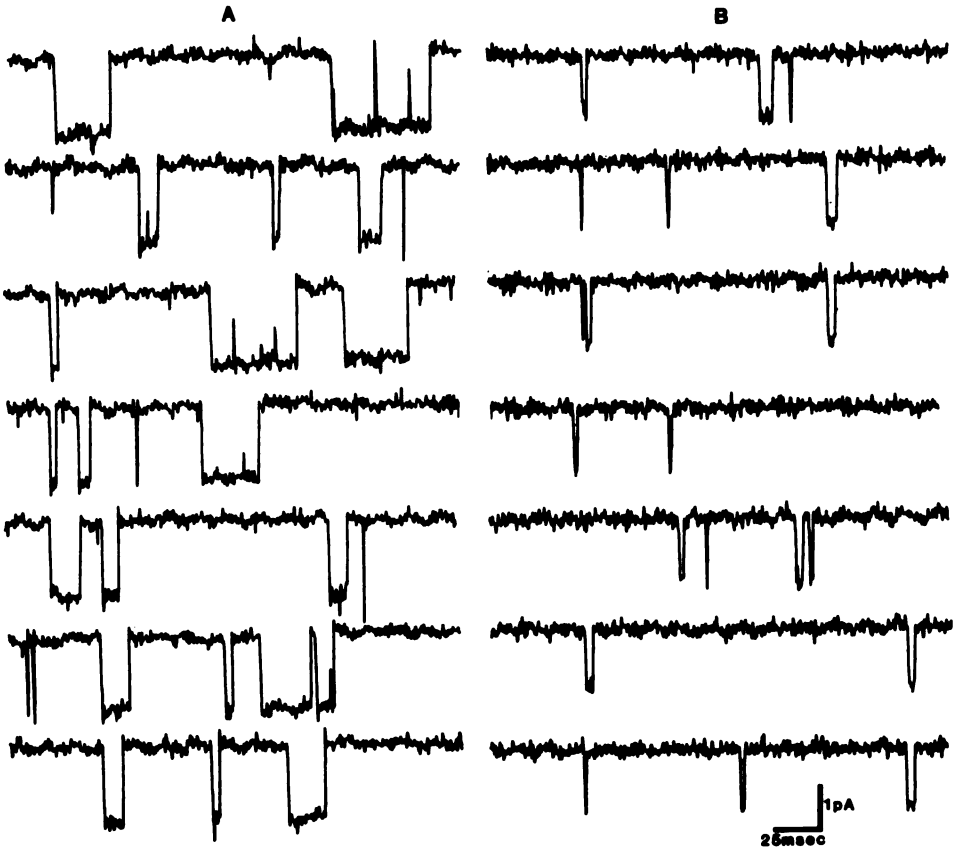

FIG. 8. *Patch clamp records of AChR currents under control condition (A) and in the presence of 10 μM TPMP (B)*

The patch electrode, sealed to a rat myoball, was held at +30 to +40 mV with respect to ground for both conditions. A, the patch pipette contained only ACh (100 nM); B, both ACh (100 nM) and TPMP (10 μM). The bandwidth was 1 kHz. Notice the shorter channel lifetime seen when TPMP was present (B).

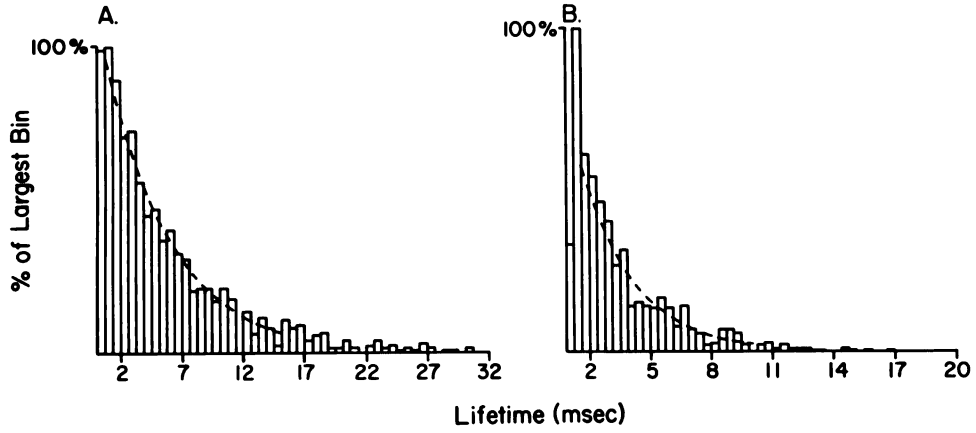

FIG. 9. *Open time histograms for single ACh channels in the presence of ACh (100 nM) only (A) and in the presence of ACh plus 10 μM TPMP (B)*

Both recordings were of excised (inside out) patches taken from the same cell; the pipette potential was + 50 mV in both recordings. 1156 channel openings are represented in A and 949 in B.

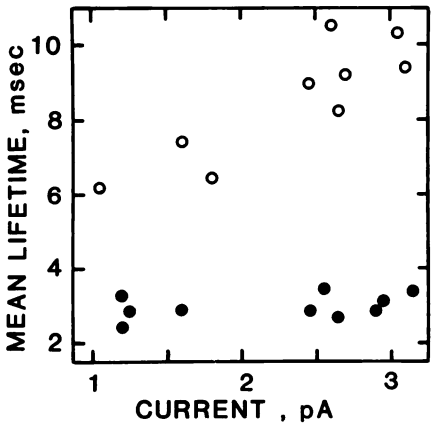

FIG. 10. *Arithmetic means of channel lifetime, obtained from patch clamp experiments under control conditions (○) and in the presence of 10 μM TPMP (●)*

Since these results were obtained under both cell-free and cell-attached conditions and since membrane potential was not known with certainty, channel currents were taken as an estimator of membrane potential. These results were obtained from 5 cells and represent totals of 10,304 channel openings under control condition and 6974 openings in the presence of TPMP.

three forms: 1) an equilibrium level that was independent of activation of the AChR but that was dependent on membrane potential; 2) a use-dependent blockade in which repetitive activation of the receptor by trains of microiontophoretic pulses of ACh produced diminishing responses; and 3) union of TPMP with the open ion channel to interrupt the current flow. We shall consider each of these findings in turn.

The equilibrium blockade increased with the concentration of TPMP and as the membrane became more hyperpolarized. Peak amplitude of EPCs elicited at 1 Hz were taken as a measure of this blockade (Fig. 4). Though the decrease in channel lifetime could account for some decrease in peak amplitude, the voltage jumps (Fig. 5) controlled for this by showing that, after a brief excursion to a different potential, peak amplitudes were changed on return to the starting potential while τ for EPC decays were not (Fig. 4). Recent biochemical studies show that the AChR exists in equilibrium with its desensitized state. About 20% of the AChR are desensitized under resting conditions in membranes isolated from *Torpedo* electric organs (e.g., Refs. 18 and 19). TPMP seemed to shift this equilibrium toward the desensitized state. The equilibrium level of blockade could correspond to AChRs thus desensitized. The topographical site on the AChR to which TPMP binds to cause this shift is not known but three classes have been identified by Heidmann *et al.* (18). These are: 1) a high affinity site, most likely within the ion channel, having a stoichiometry of one site per AChR complex; 2) the protein-lipid interface; and 3) nonsaturating sites in bulk lipid. After a step change in membrane potential, the blockade followed an exponential time course (Fig. 4) which could correspond to the shift

$$R + D \rightarrow RD \rightarrow R'D$$

in which R represents the AChR, D represents TPMP, and R' represents the desensitized AChR. Since single exponential relaxations were seen, one step is rate limiting. Plots of relaxation constant versus TPMP concentration could yield kinetic parameters and, if high enough concentration of TPMP could be used, indicate which step is rate limiting. Unfortunately, one cannot maintain a single fiber under voltage clamp long enough to test several concentrations.

The AChR was activated by microiontophoretic pulses of ACh and by nerve stimulation (EPCs). Both methods showed diminished peak amplitudes when TPMP was present. Though we showed that TPMP did not alter quantal content, the microiontophoretic method, in bypassing the nerve, showed decisively that the blockade was postsynaptic and that it deepened with increasing TPMP concentration and with increasing frequency of ACh pulses (Fig. 3). The trains of ACh response were complicated by an initial facilitation followed by a double exponential decay ("rundown") that approached an asymptote. Models to accommodate these results would have too many free parameters to provide insight into mechanisms. It was useful, however, to consider the

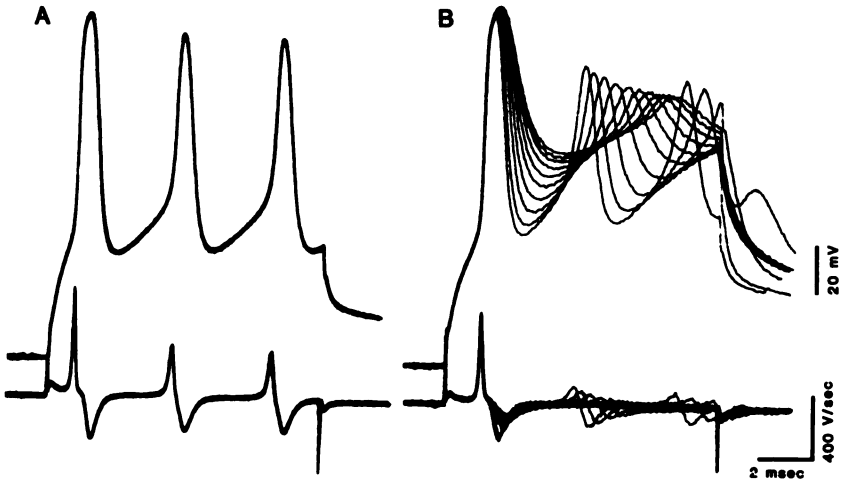

FIG. 11. *Trains of 10 action potentials (1 Hz) under control condition (A) and in the presence of 100 μM TPMP (B)*
The sartorius muscles were mildly glycerol shocked (200 mM glycerol, 1 hr) to reduce the force of the twitch. Lower traces are first derivatives of the voltage traces above. Resting membrane potentials were −95 mV. Cells were hyperpolarized to −100 mV before they were depolarized to threshold.

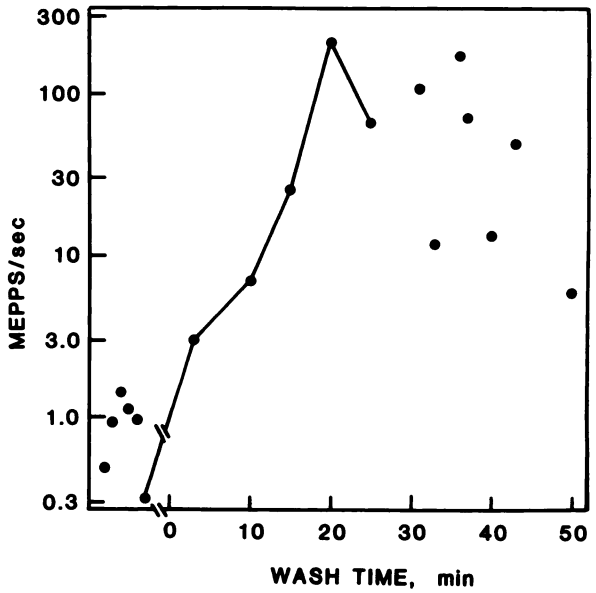

FIG. 12. *MEPP frequency before and after treatment with TPMP*
MEPP frequency was estimated in six fibers (points before the break). Impalement of the sixth fiber was maintained during the treatment with TPMP (100 μM, 1 hr) and during the washout time points connected by the line. All points not connected are estimates from separate fibers of the same muscle. The data shown were compiled from a total of 6676 MEPPS.

simplest scheme (Appendix) which showed, for a *constant* fractional blockade of available receptors that recover by an exponential time course, that 1) even a small fractional block can produce a high cumulative block at high frequencies, and 2) that the rate constant for the envelope of declining ACh potentials depends on the fractional blockade and the rate constant for recovery from blockade. Whereas under control conditions rundown was slight (10%) or nonexistent, concentrations of TPMP as low as 0.5 μM could produce over 50% rundown. These experiments showed that, apart from the equilibrium level of blockade, ACh exposed a new pathway(s) to the blocked states. One of the pathways for which we have evidence is binding of TPMP to the open conformation of the AChR. This is the familiar sequential model for open channel blockade (e.g., Refs. 1–3) in which TPMP enters the open channel and, upon binding, prevents further current flow until TPMP dislodges. If the reverse of this process is slow, EPC decays remain single exponential functions of time with rate constants proportional to the TPMP concentration. Such results were seen (Figs. 6 and 7), and direct recordings of single channels confirmed that lifetimes were shortened (Figs. 8–10). Whereas this reaction blocks the channel, we have no evidence bearing on its contribution to the blocked states revealed by the rundown experiments. Neher's (20) careful study of the open channel blockade by QX222 revealed that the blocked receptors do not always retrace their steps back through the open state, as required in the sequential model. TPMP, after binding to the open channel, may promote a conformation change in the AChR to a desensitized state. Other lines of evidence show that activation can lead to an intermediate state that is neither the open channel conformation nor the slowly approached, desensitized one (21–23). Electrophysiological studies support this conclusion. For example, meproadifen (12, 24) nortriptyline (25), and phenothiazines (26) profoundly promote desensitization without shortening EPC time constants. Thus, in the presence of ACh and TPMP, the AChR may exist in four (or perhaps more) states, a resting, an open, and two blocked states, and even the simplest schemes involving these will yield the multiexponential kinetics for recovery revealed by the rundown experiments (Fig. 2). A route we can exclude is one in which, after blockade of the open channel, the AChR oscillates between an intermediate state and back to the open state. Such oscillation should, if fast enough, appear as "bursts" of openings in the patch clamp experiments. We observed no such bursts; channel lifetimes simply became shorter (Figs. 8–10).

How do our findings correspond to the uptake studies?

The binding studies clearly show that, in *Torpedo* at least, TPMP does not compete with ACh for its recognition site (4), so competitive blockade is excluded. Both approaches agree that agonists enhance the blockade, but the time course revealed by the biochemical studies is on the order of seconds or minutes even when relatively high concentrations of TPMP and carbamylcholine were used (4, 6). Its binding, with $K_d = 1.5\ \mu M$ (4), may correspond to the high affinity site identified by Heidmann *et al.* (18).

Heidmann *et al.* (18) also identified low affinity and nonsaturable binding sites for noncompetitive blocking agents. These sites correspond to the AChR-lipid interface and bulk lipids, respectively. Since TPMP is a hydrophobic cation (see references in Refs. 4 and 5), we must assume that it, too, can act, at least in part, through these sites. Indeed a spin-labeled analogue of TPMP that is associated *exclusively* with membranes has been shown to slow its diffusion (presumably by binding to the AChR) when an agonist is present (8). This result suggested that the TPMP analogue could finds its blocking site on the AChR via the membrane. Perhaps perturbations by TPMP at lipid-protein interfaces may be responsible for its effects on action potentials (Fig. 11). The permeability of TPMP through membranes may also permit access to intracellular sites in the presynaptic nerve terminal and, by releasing stores of calcium, cause the increase in MEPP frequency.

ACKNOWLEDGMENTS

We are indebted to Dr. Mohammed Maleque for performing some of the EPC experiments and we are grateful to Ms. Mabel Zelle and Ms. Lauren Aguayo for their cheerful diligence in analyzing the EPC and patch clamp data.

APPENDIX

In this scheme for the blockade of the AChR that ensues during repetitive stimulation by the agonist, we assume that each pulse of the agonist blocks a constant fraction, f, of the available AChRs, and that these AChRs unblock as a first order reaction with rate constant k. The measured response is proportional to the number of free receptors, R. Initially there are R_1 free receptors. The pulse interval is the constant, t. At time t after the first pulse, just preceding the second pulse, the number of blocked receptor, r_1, is

$$r_1 = fR_1e^{-kt}$$

so that the number of free receptors at this time is

$$R_2 = R_1 - r_1 = R_1(1 - fe^{-kt})$$

At the time preceding the third pulse, the number of blocked receptors is

$$r_2 = fR_2e^{-kt} + fR_1e^{-2kt}$$

$$r_2 = fR_1e^{-kt}[1 + e^{-kt}(1 - f)]$$

In general one finds that

$$r_n = fR_1e^{-kt}\left[\sum_{j=0}^{n-1} e^{-jkt}(1 - f)^j\right]$$

and the number of free receptors is

$$R_{n+1} = R_1 - r_n$$

The asymptotic ratio of free receptors to those free at the first pulse is then

$$\frac{R_\infty}{R_1} = \frac{1 - e^{-kt}}{1 - e^{-kt}(1 - f)}$$

because

$$\sum_{j=0}^{\infty} e^{-jkt}(1 - f)^j = [1 - e^{-jkt}(1 - f)^j]^{-1}$$

This is the result used for Fig. 3. After subtracting the asymptote, R_∞, the ratio of successive response is

$$\frac{R_{n+1} - R_\infty}{R_n - R_\infty} = e^{-kt}(1 - f)$$

REFERENCES

1. Spivak, C. E., and E. X. Albuquerque. The dynamic properties of the nicotinic acetylcholine receptor ionic channel complex: activation and blockade, in *Progress in Cholinergic Biology: Model Cholinergic Synapses* (I. Hanin and A. M. Goldberg, eds.). Raven Press, New York, 323–357 (1982).
2. Albuquerque, E. X., M. Adler, C. E. Spivak, and L. Aguayo. Mechanism of nicotinic channel activation and blockade. *Ann. N. Y. Acad. Sci.* **358**:204–238 (180).
3. Peper, K., R. J. Bradley, and F. Dreyer. The acetylcholine receptor at the neuromuscular junction. *Physiol. Rev.* **62**:1271–1340 (1982).
4. Lauffer, L. and F. Hucho. Triphenylmethylphosphonium is an ion channel ligand of the nicotinic acetylcholine receptor. *Proc. Natl. Acad. Sci. U.S.A.* **79**:2406–2409 (1982).
5. Muhn, P., and F. Hucho. Covalent labeling of the acetylcholine receptor from *Torpedo* electric tissue with the channel blocker [^{3}H]triphenylmethylphosphonium by ultraviolet irradiation. *Biochemistry* **22**:421–425 (1983).
6. Muhn, P., A. Fahr, and F. Hucho. Photoaffinity labeling of acetylcholine receptor in millisecond time scale. *FEBS Lett.* **166**:146–150 (1984).
7. Tsai, M.-C., E. X. Albuquerque, R. S. Aronstam, A. T. Eldefrawi, M. E. Eldefrawi, and D. J. Triggle. Sites of action of phencyclidine. I. Effects on the electrical excitability and chemosensitive properties of the neuromuscular junction of skeletal muscle. *Mol. Pharmacol.* **18**:159–166 (1980).
8. Cafiso, D. S. Paramagnetic hydrophobic ions as probes for electrically active conformational transitions in ion channels. *Biophys. J.* **45**:6–7 (1984).
9. Davis, C. G., S. Hestrin, H. Landahl, A. S. Gordon, I. Diamond, and J. I. Korenbrot. Activation of acetylcholine receptors causes the partition of hydrophobic cations into postsynaptic membrane vesicles. *Nature* **302**:525–528 (1983).
10. Gage, P. W., and R. S. Eisenberg. Action potentials without contraction in frog skeletal muscle fibers with disrupted transverse tubules. *Science* (*Wash. D. C.*) **158**:1702–1703 (1967).
11. Kuba, K., E. X. Albuquerque, J. Daly, and E. A. Barnard. A study of the irreversible cholinesterase inhibitor, diisopropylfluorophosphate, on time course of end-plate currents in frog sartorius msucle. *J. Pharmacol. Exp. Ther.* **189**:499–512 (1974).
12. Maleque, M. A., C. Souccar, J, B. Cohen, and E. X. Albuquerque. Meproadifen reaction with the ionic channel of the acetylcholine receptor: potentiation of agonist-induced desensitization at the frog neuromuscular junction. *Mol. Pharmacol.* **22**:636–647 (1982).
13. Spivak, E. C., M. A. Maleque, A. C. Oliveira, L. M. Masukawa, T. Tokuyama, J. W. Daly, and E. X. Albuquerque. Actions of the histrionicotoxins at the ion channel of the nicotinic acetylcholine receptor and at the voltage-sensitive ion channels of muscle membranes. *Mol. Pharmacol.* **21**:351–361 (1982).
14. A. Akaike, S. R. Ikeda, N. Brookes, G. J. Pascuzzo, D. L. Rickett, and E. X. Albuquerque. The nature of the interactions of pyridostigmine with the nicotinic acetylcholine receptor ioic channel complex. II. Patch clamp studies. *Mol. Pharmacol.* **25**:102–112 (1984).
15. Daniels, F., J. W. Williams, P. Bender, R. A. Alberty, and C. D. Cornwell. *Experimental Physical Chemistry*. McGraw-Hill, New York, 140–141 (1962).
16. Anderson, C. R., and C. F. Stevens. Voltage clamp analysis of acetylcholine produced end-plate current fluctuations at frog neuromuscular junction. *J. Physiol.* (*Lond.*) **235**:655–691 (1973).
17. Narahashi, T., T. Deguchi, N. Urakawa, and Y. Ohkubo. Stabilization and rectification of muscle fiber membrane by tetrodotoxin. *Am. J. Physiol.* **198**:934–938 (1960).
18. Heidmann, T., R. E. Oswald, and J.-P Changeux. Multiple sites of action for noncompetitive blockers on acetylcholine receptor rich membrane fragments from *Torpedo marmorata*. *Biochemistry* **22**:3112–3127 (1983).
19. Cohen, J. B., N. D. Boyd, and N. S. Shera. Interactions of anesthetics with nicotinic postsynaptic membranes isolated from *Torpedo* electric tissue, in

Progress in Anesthesiology (B. R. Fink, ed.), Vol. 2. Raven Press, New York, 165–175 (1980).
20. Neher, E. The charge carried by single-channel currents of rat cultured muscle cells in the presence of local anaesthetics. *J. Physiol.* (*Lond.*) **339**:663–678 (1983).
21. Neubig, R. R., and J. B. Cohen. Permeability control by cholinergic receptors in *Torpedo* postsynaptic membranes: agonist dose-response relations measured at second and millisecond times. *Biochemistry* **19**:2770–2779 (1980).
22. Heidmann, T., and J.-P Changeux. Interaction of a fluorescent agonist with the membrane-bound acetylcholine receptor from Torpedo marmorata in the millisecond time range: resolution of an "intermediate" conformational transition and evidence for positive cooperative effects. *Biochem. Biophys. Res. Commun.* **97**:889–896 (1980).
23. Magleby, K. L., and B. S. Pallotta. A study of desensitization of acetylcholine receptors using nerve-related transmitter in the frog. *J. Physiol.* (*Lond.*) **316**:225–250 (1981).
24. Aracava, Y., S. R. Ikeda, and E. X. Albuquerque. Meproadifen enhances activation and desensitization of the acetylcholine receptor ionic channel complex (AChR): single channel studies. *Abstr. Neurosci.* **9**:733 (1983).
25. Schofield, G. G., B. Witkop, J. E. Warnick, and E. X. Albuquerque. Differentiation of the open and closed states of the ionic channels of nicotinic acetylcholine receptors by tricyclic antidepressants. *Proc. Natl. Acad. Sci. U. S. A.* **78**:5240–5244 (1981).
26. Carp, J. S., R. S. Aronstam, B. Witkop, and E. X. Albuquerque. Electrophysiological and biochemical studies on enhancement of desensitization by phenothiazine neuroleptics. *Proc. Natl. Acad. Sci. U. S. A.* **80**:310–314 (1983).

Send reprint requests to: Dr. E. X. Albuquerque, Department of Pharmacology and Experimental Therapeutics, University of Maryland School of Medicine, 660 West Redwood Street, Baltimore, MD 21201